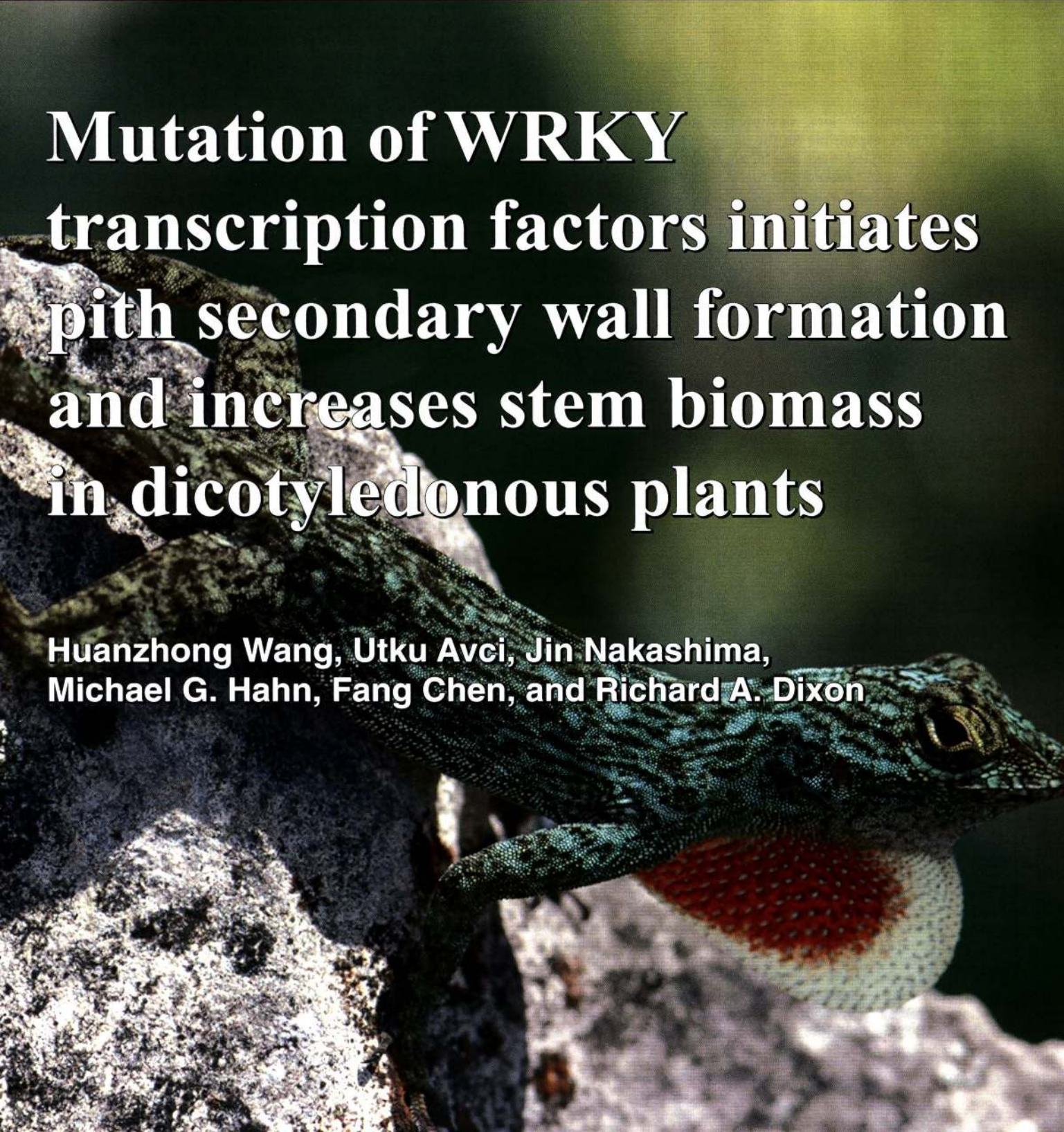


Mutation of WRKY transcription factors initiates pith secondary wall formation and increases stem biomass in dicotyledonous plants

**Huanzhong Wang, Utku Avcı, Jin Nakashima,
Michael G. Hahn, Fang Chen, and Richard A. Dixon**



Mutation of WRKY transcription factors initiates pith secondary wall formation and increases stem biomass in dicotyledonous plants

Huanzhong Wang^a, Utku Avci^{b,c}, Jin Nakashima^a, Michael G. Hahn^{b,c}, Fang Chen^{a,c}, and Richard A. Dixon^{a,c,1}

^aPlant Biology Division, Samuel Roberts Noble Foundation, Ardmore, OK 73401; ^bComplex Carbohydrate Research Center, University of Georgia, Athens, GA 30602; and ^cBioenergy Sciences Center (BESC), Oak Ridge, TN 37831

Contributed by Richard A. Dixon, November 4, 2010 (sent for review September 22, 2010)

Stems of dicotyledonous plants consist of an outer epidermis, a cortex, a ring of secondarily thickened vascular bundles and interfascicular cells, and inner pith parenchyma cells with thin primary walls. It is unclear how the different cell layers attain and retain their identities. Here, we show that WRKY transcription factors are in part responsible for the parenchymatous nature of the pith cells in dicotyledonous plants. We isolated mutants of *Medicago truncatula* and *Arabidopsis thaliana* with secondary cell wall thickening in pith cells associated with ectopic deposition of lignin, xylan, and cellulose, leading to an ~50% increase in biomass density in stem tissue of the *Arabidopsis* mutants. The mutations are caused by disruption of stem-expressed WRKY transcription factor (TF) genes, which consequently up-regulate downstream genes encoding the NAM, ATAF1/2, and CUC2 (NAC) and CCCH type (C3H) zinc finger TFs that activate secondary wall synthesis. Direct binding of WRKY to the NAC gene promoter and repression of three downstream TFs were confirmed by *in vitro* assays and in planta transgenic experiments. Secondary wall-bearing cells form lignocellulosic biomass that is the source for second generation biofuel production. The discovery of negative regulators of secondary wall formation in pith opens up the possibility of significantly increasing the mass of fermentable cell wall components in bioenergy crops.

lignocellulosic bioenergy crops | transcriptional regulation | lignin modification | biomass yield

In dicotyledonous plants, the stem structure in cross-section is organized into (from outer to inner) the epidermis, the cortex, a ring of vascular bundle cells and interfascicular tissues characterized by secondary wall thickening, and the parenchymatous pith cells with thin primary cell walls. The different cell layers are well-defined and manifest distinct functions. How these cells attain and retain their identities is still unclear.

The secondary cell walls of mature plants comprise a large proportion of the lignocellulosic biomass used as starting material for second generation biofuel production (1, 2). The synthesis of secondary cell wall components is highly coordinated and regulated by ordered transcriptional switches (3, 4). Several closely related NAC transcription factors (TFs) act as master regulators (5–9). MYB domain TFs, either upstream (10) or downstream (11) of NAC TFs, may also function as master switches, and farther downstream, TFs directly interact with cellulose, lignin, and xylan biosynthesis genes (12, 13).

Forward genetic mutant screening is a powerful tool to identify players in a given biological process. Screening for ectopic lignification mutants in *Arabidopsis* has identified two mutants that show lignified pith cells (14, 15), but neither mutation defines a negative transcriptional regulator of lignin synthesis as originally proposed (16, 17). In this study, we report the identification and characterization of *Medicago* and *Arabidopsis* mutants showing ectopic secondary cell wall formation in pith cells. The mutant phenotypes are caused by disruption of WRKY TFs, which function to maintain pith cells in their parenchymatous state by repressing downstream NAC and C3H zinc finger TFs that control xylan, cellulose, and lignin formation. Loss of func-

tion of the WRKY TFs, therefore, results in a significant increase in stem biomass.

Results

Identification of a *Medicago* Mutant with Secondary Wall Formation in Pith Cells. To identify genes that control secondary cell wall formation, we screened an *M. truncatula Tnt1* retrotransposon insertion population (18, 19) by UV microscopy of stem sections (8). Mutant line NF3788 showed ectopic lignin autofluorescence in pith cells, with the strongest phenotype in mature internodes (Fig. 1A). Phloroglucinol and Mäule staining (Fig. 1B and C and Fig. S1A) confirmed progressive ectopic lignification into the pith with increasing stem maturity in the mutant. Furthermore, the red color of the Mäule staining suggested a high syringyl (S) lignin content in the pith cell walls, which was confirmed by thioacidolysis (20). Although the total lignin in the stem of the mutant was only slightly increased, lignin levels were double in isolated pith material, with a fourfold higher level of S lignin units than in pith from WT plants (Fig. 1D).

The walls of the lignified pith cells in the mutant were significantly thicker than in the WT (Fig. 1E and F). Secondary walls are primarily composed of lignin, xylan (hemicellulose), and cellulose. We, therefore, checked the lignified pith cells for the presence of xylan by immunohistochemistry using three distinct xylan-directed antibodies (21) and for the presence of cellulose using the cellulose-directed carbohydrate-binding module (CBM) 2a (22). The results confirmed that the pith cell walls in the mutant had undergone true secondary thickening as opposed to only lignification (Fig. 1G and H). We, therefore, named the mutant secondary wall thickening in pith (*mtstp-1*).

MtSTP Gene Encodes a WRKY Transcription Factor. To identify the gene responsible for the STP phenotype, microarray analysis was performed using RNA isolated from the fourth to eighth internodes of control and mutant plants in a segregating population. Fifty-seven probe sets were down-regulated in the mutant line by at least two-fold (Table S1), and candidate genes were selected based on their level of down-regulation and stem preferential expression in the *Medicago* Gene Expression Atlas (23). One candidate, Mtr.5137.1.S1_at, contained a *Tnt1* insertion that cosegregated with the ectopic lignification phenotype. Using the Mtr.5137.1.S1_at probe sequence to search against the *M. truncatula* databases at <http://www.medicago.org/>, we identified the putative coding sequence of *MtSTP*, part of which was identical to IMGAIAC202489_11.1.

Author contributions: H.W., F.C., and R.A.D. designed research; H.W., U.A., J.N., M.G.H., and F.C. performed research; H.W. and R.A.D. analyzed data; and H.W. and R.A.D. wrote the paper.

The authors declare no conflict of interest.

Data deposition: The sequences reported in this paper have been deposited in the GenBank database [accession nos. HM622066 (*MtSTP* genomic) and HM622067 (coding)], and the microarray data reported in this paper have been deposited in MIAMEXpress database (<http://www.ebi.ac.uk/miamexpress/>) (accession nos. E-MEXP-2792 and E-MEXP-2793).

¹To whom correspondence should be addressed. E-mail: radixon@noble.org.

This article contains supporting information online at www.pnas.org/lookup/suppl/doi:10.1073/pnas.1016436107/-DC5Supplemental.

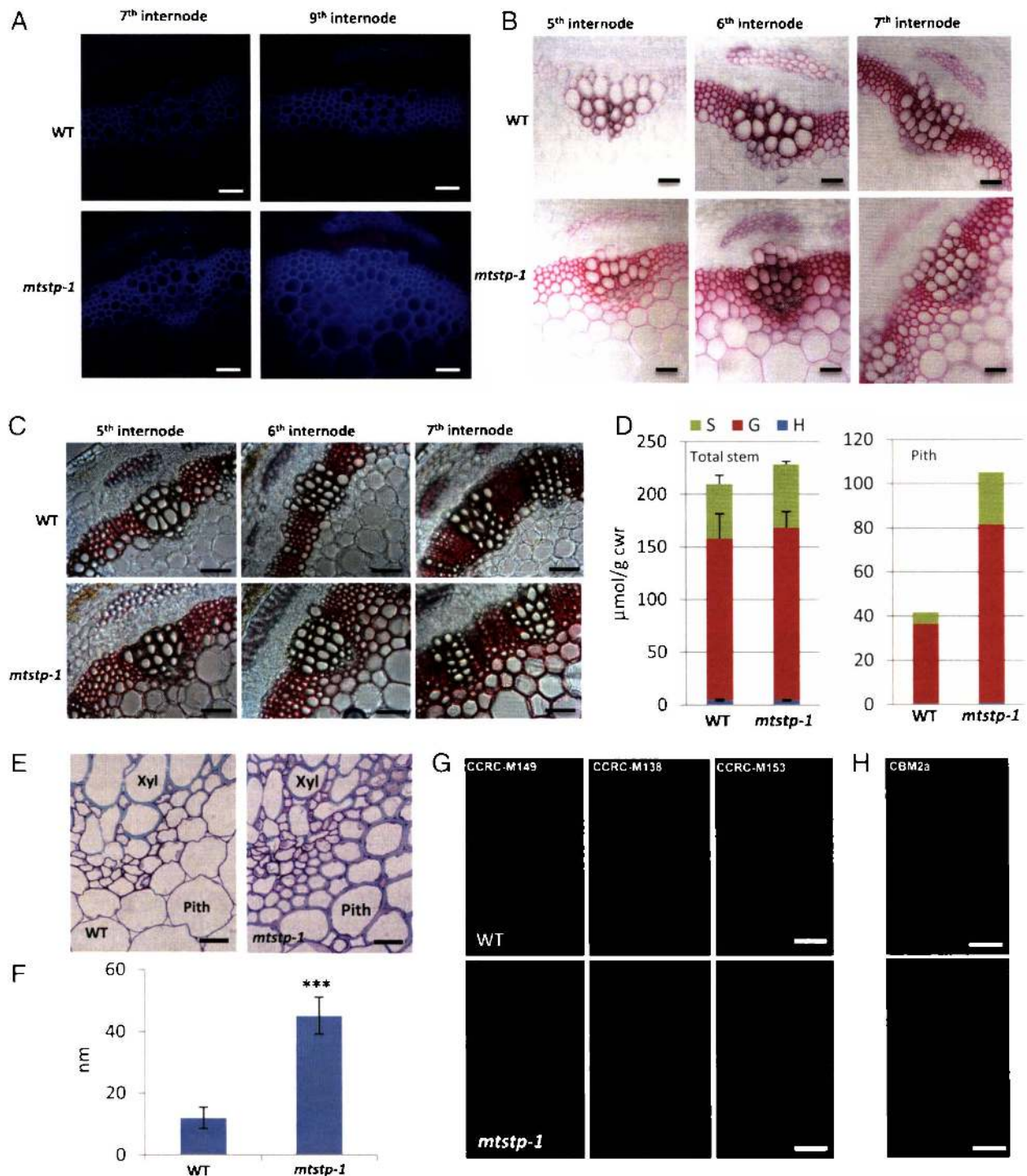


Fig. 1. Phenotypic analysis of the *Mtstp-1* mutant. (A) UV autofluorescence of cross-sections of the seventh and ninth internodes. The blue color is lignin autofluorescence in vascular bundles and interfascicular fibers. Lignification first extends to pith cells near the bundle and then to the central part in older internodes. (B) Phloroglucinol staining of the fifth, sixth, and seventh internodes of stems from WT plants and *Mtstp-1* mutant. (C) Mäule staining of the fifth, sixth, and seventh internodes of stems from WT plants and the *Mtstp-1* mutant. (D) Lignin content and composition determined by thioacidolysis. (Left) Total stem; error bars represent SD. (Right) Isolated pith. (E) Light microscopy of pith cell walls in WT and mutant. (F) Quantification of cell wall thickness of the WT and mutant sections; error bars represent \pm SD (asterisks indicate a highly significant *t* test score; $n = 30$, $P < 0.0001$). (G and H) Detection of xylan and cellulose by immunohistochemistry using monoclonal antibodies against distinct xylan epitopes (G) and a carbohydrate-binding module that binds crystalline cellulose (H) in stem sections of WT (Upper) and *Mtstp-1* mutant (Lower). Antibody and CBM names are indicated in G Upper and H Upper. (Scale bar: A–C and E, 20 μ m; G and H, 10 μ m.)

We then cloned the corresponding genomic sequence, which contained four exons and three introns. The *Tnt1* insertion was located at the far 3' end of the last intron, which was confirmed by RT-PCR (Fig. 2A and B). There was no *MtSTP* transcript detected

in the mutant (Fig. 2C). *MtSTP* encodes a WRKY family TF that is preferentially expressed in stem internodes, where its transcript level increases with maturity (Fig. 2D) but is not influenced by hormones or biotic or abiotic stress (Fig. S1B).

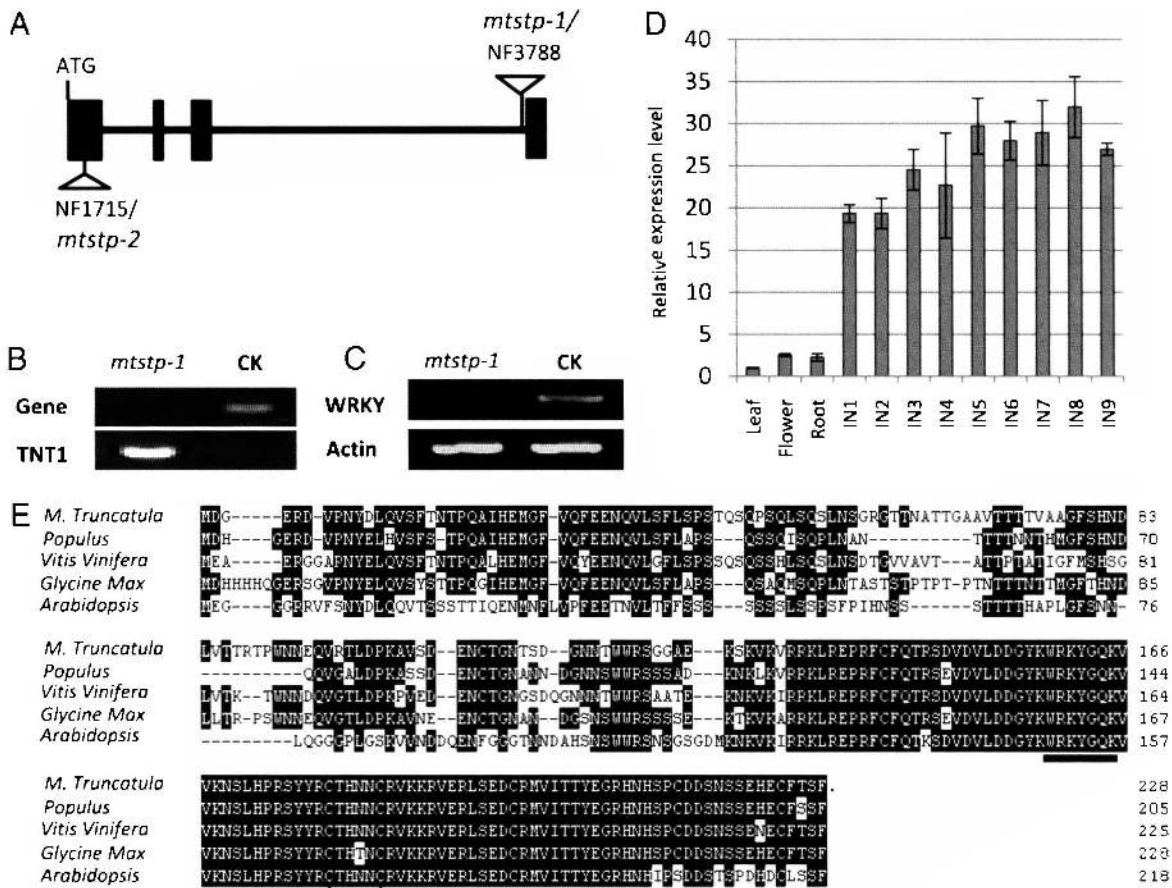


Fig. 2. Molecular cloning of *MtSTP* and alignment with homologous proteins. (A) *MtSTP* gene structure and *Tnt1* insertion site. (B) PCR identification of homozygotes of the *Tnt1* insertion line; the WT plant has only a gene-specific band, whereas the insertion line has only a T-DNA-specific band. (C) RT-PCR analyses of *MtSTP* transcript levels using primers covering the full-length cDNA. *ACTIN* was used as control. (D) Quantitative (q) RT-PCR showing expression of *MtSTP* in different organs (IN, internode) normalized to expression of *ACTIN*. Bars represent \pm SD. (E) Alignment with homologous proteins. Black shading indicates identical amino acids. The conserved WRKY domain and C2H2 zinc finger motif are marked by a line and triangles, respectively.

To confirm that the STP phenotype was caused by the *Tnt1* disruption in *MtSTP*, we used *MtSTP* gene-specific primers for reverse genetic screening of DNA pools from the *Tnt1* mutant population, and another insertion line, NF1715/*mtstp-2*, was recovered with a similar phenotype to that of *mtstp-1* (Fig. S1D).

Identification of Arabidopsis Mutants Showing the STP Phenotype. Several related WRKY proteins were identified from *Populus trichocarpa*, *Vitis vinifera*, *Glycine max*, and *A. thaliana* (*AtWRKY-12/At2g44745*). They all contained a conserved WRKYGQK motif and a C2H2 zinc finger sequence at their C termini (Fig. 2E). Two lines predicted to have transfer (T)-DNA insertions in the *AtWRKY-12* gene were obtained from the Arabidopsis Biological Resource Center (24), and PCR and sequencing confirmed that both lines harbored an insertion in the last intron of the gene (Fig. S2A and B). Homozygous plants of both *wrky12-1* and *wrky12-2* showed reduced transcript abundance of *AtWRKY12* (Fig. S2C) and similar lignin phenotypes to *mtstp* mutants (Fig. S2D and E).

The walls of some pith cells in the *wrky12* mutants underwent secondary thickening as shown by transmission EM (Fig. 3A) and similar to *Medicago mistp-1* plants, contained deposits of xylan and crystalline cellulose that appeared indistinguishable from those in the secondary walls of adjacent xylem cells (Fig. S3B and C). *AtWRKY-12* and *MtSTP* are, thus, true homologs that function in controlling pith cell wall formation in *Medicago* and *Arabidopsis*, respectively. We measured the diameters and dry weights of *wrky12-1* stems and found significantly increased biomass

density (Fig. 3B), presumably as a result of the increased deposition of cell wall material. This did not seem to occur at the expense of the development of other plant organs, because whole-plant above-ground biomass was also significantly increased by ~25% in the mutant plants (Fig. S3A) and mutations in these genes have little impact on overall plant growth (Fig. S4).

Complementation of *wrky12-1* with *AtWRKY12* and *MtSTP*. To confirm that the STP phenotype was indeed caused by disruption of the *AtSTP* gene, we performed complementation with two genetic strategies. First, the WT *AtWRKY-12* genomic sequence, including a 1.88-kb promoter sequence and 458-bp 3' untranslated sequence, was introduced into homozygous *wrky12-1* mutant plants. Of 72 phosphinothricin (BASTA)-resistant T1 transformants, 62 exhibited a restored WT phenotype (Fig. 3C and D). In addition, a 35S:*AtWRKY12-YFP* fusion was transformed into the *wrky12-1* background; 7 of 36 transformants showed retarded growth, some being extremely small and unable to set seed (Fig. 3E and F). However, the lignin UV autofluorescence pattern of stem sections was more normal, although the stems were much thinner than WT (Fig. 3G-I). Thus, *AtWRKY12* is responsible for the STP phenotype. Homozygous *wrky12-1* plants were also transformed with a 35S:*MtSTP* construct, and 16 of 37 transgenic T1 plants were restored to the WT phenotype, indicating conserved functions for the homologous *Medicago* and *Arabidopsis* STP genes.

Expression Pattern and Subcellular Localization of *AtWRKY12*. Consistent with the expression pattern of *MtSTP*, *AtWRKY12* is also

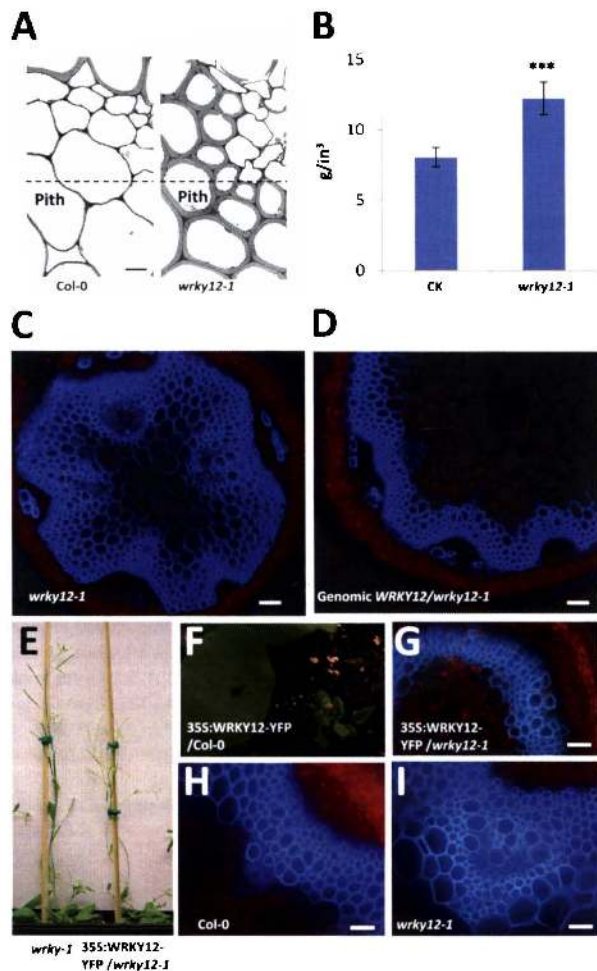


Fig. 3. Phenotypes and complementation of the Arabidopsis *wrky12* mutant. (A) Transmission electron microscopy (TEM) showing pith cell wall thickness of WT Arabidopsis and the *wrky12-1* mutant. Each panel was constructed from two contiguous TEM fields; their points of assembly are indicated by the dashed lines. (B) Comparison of the biomass density in stems of *wrky12-1* mutant and control (CK; asterisks indicate highly significant values as determined by *t* test; $P < 0.0001$). (C and D) UV autofluorescence of stem cross-sections of *wrky12-1* (C) and *wrky12-1* transformed with the genomic complementation construct (D). (E) Visible phenotypes. The *wrky12-1* mutant plant is on the left, and *35S:AtWRKY12-YFP* transformant in the mutant background is on the right. (F) Phenotype of a *35S:AtWRKY12-YFP* overexpressor (Right) compared to wild-type (Left). (G) UV autofluorescence of a stem section showing complementation of the STP phenotype. (H and I) UV autofluorescence of stem sections of WT *Col-0* and *wrky12-1*. (Scale bar: C, D, and G–I, 20 μ m.)

highly expressed in stem and hypocotyls (Fig. S1C). Transformation of Arabidopsis with a *WRKY12* promoter– β -glucuronidase (GUS) reporter fusion confirmed the preferential expression in stem and hypocotyl, and no expression was detected in root and floral tissues. Stem-section staining revealed GUS activity in pith cells and cortex tissues but not vascular and interfascicular fibers (Fig. S5A–E).

Infiltration of *Nicotiana benthamiana* leaves or stable transformation of WT Arabidopsis plants with *Agrobacterium* harboring the *35S:AtWRKY12-YFP* fusion resulted in localization of YFP signal exclusively in the nucleus (Fig. S5F). Although the construct was driven by the constitutive 35S promoter, the YFP signal in stably transformed Arabidopsis was localized to nuclei of root epidermis and hairs on mature roots. There was no signal in the root meristem or root elongation zone (Fig. S5G and H), suggesting that the stability of the protein is developmentally controlled.

Mechanism of WRKY Function in Pith Cell Wall Formation. Microarray analysis indicated that 52 and 44 genes are up-regulated and 95 and 286 genes are down-regulated, more than twofold, in the *wrky12-1* and *wrky12-2* mutants, respectively (Table S1B). Among the up-regulated genes, a considerable number are related to secondary cell wall synthesis, including two C3H zinc finger TFs and the NAC domain TF NST2, which, like *AtWRKY12*, are most highly expressed in stem tissue (Fig. S6). *AtNST2* regulates secondary wall thickening in anther endothecium (6), and *AtC3H14* (At1g66810) has been reported to be a transcriptional activator of secondary wall synthesis in an in vitro assay (25).

To test if expression of *NST2* and the two C3H zinc finger TFs are up-regulated in pith cells after loss of *AtWRKY12* function, we isolated vascular and pith tissues from WT and *wrky12-1* mutant plants. Quantitative RT-PCR analysis showed that these three TFs are highly expressed in cells with secondarily thickened walls and barely up-regulated in vascular tissues of the *wrky12-1* mutant, but they are significantly up-regulated in pith cells of the mutant (Fig. S6). Genes responsible for secondary wall component synthesis were found to be up-regulated in the mutant line from microarray analyses (Table S1C), and overexpression of lignin biosynthetic genes in the mutant pith cells was confirmed by quantitative RT-PCR analyses (Fig. S6). Thus, *AtWRKY12* controls cell fate in pith cells by acting as a negative regulator of *NST2* and C3H zinc finger TFs, which, in turn, regulate secondary cell wall synthesis.

To directly show that STP proteins can repress the expression of these two classes of TFs, *35S:STP* effector constructs and reporter constructs, in which the promoter sequences of *NST2* or the two C3H TFs were placed in front of the firefly luciferase gene (Fig. 4A), were cotransformed into *Arabidopsis* leaf protoplasts. Coexpression of *AtWRKY12* or *MtSTP* down-regulated expression of all three reporters by about 10-fold compared with empty vector controls (Fig. 4B). To test if such repression also takes place in planta, we overexpressed *AtWRKY12* in the *Col-0* and *wrky12-1* backgrounds (Fig. 4C). This led to down-regulation of *NST2* and the two C3H zinc finger TF genes in both backgrounds (Fig. 4D).

The promoters of *NST2* and both C3H zinc finger TFs contain a conserved W-box TTGACT/C motif, which can be bound by WRKY TFs. EMSA using heterologously expressed *AtWRKY12* protein revealed that *AtWRKY12* could bind directly to the *NST2* promoter fragment (Fig. 4E) but not to the promoters of the two C3H zinc finger TFs (Fig. S7).

Discussion

Pith parenchyma cells normally have thin primary walls, although they are adjacent to the ring of secondarily thickened vascular bundles and interfascicular cells. The function of WRKY TFs in maintaining pith primary wall formation in two unrelated species suggests that a conserved mechanism exists in dicotyledonous plants for confining secondary wall synthesis to specific cell types. In the vascular bundles and interfascicular tissues of WT plants, where these WRKYs are not expressed, the NAC and MYB46 TFs turn on the downstream C3H zinc finger transcription switch and other cell wall-related TFs. However, expression of NAC and MYB46 TFs is absent in pith cells (9, 11). Loss of WRKY expression in *stp* mutants leads to derepression of *NST2* and the C3H zinc finger TFs in the pith cells closest to vascular tissues and consequent activation of downstream TFs; this activation turns on the biosynthesis of the xylan, cellulose, and lignin required for secondary wall thickening to levels that can ultimately increase the stem biomass by up to 50%. Secondary wall synthesis in vascular bundles and interfascicular tissues seems unaffected in the mutant plants. The progressive spread of ectopic secondary wall formation to the center of the pith during development in the mutant plants suggests either the involvement of an additional mobile signal or limitation of carbon supply for polymer synthesis.

The *WRKY* genes are expressed in both pith and cortex, but the striking secondary cell wall formation in the *wrky* mutants is only seen in pith cells. Overexpression of *MYB83* or *MYB46* driven by the CaMV 35S promoter results in secondary wall formation in cortex but not pith cells (11, 26), but overexpression of *SND1*, the direct up-

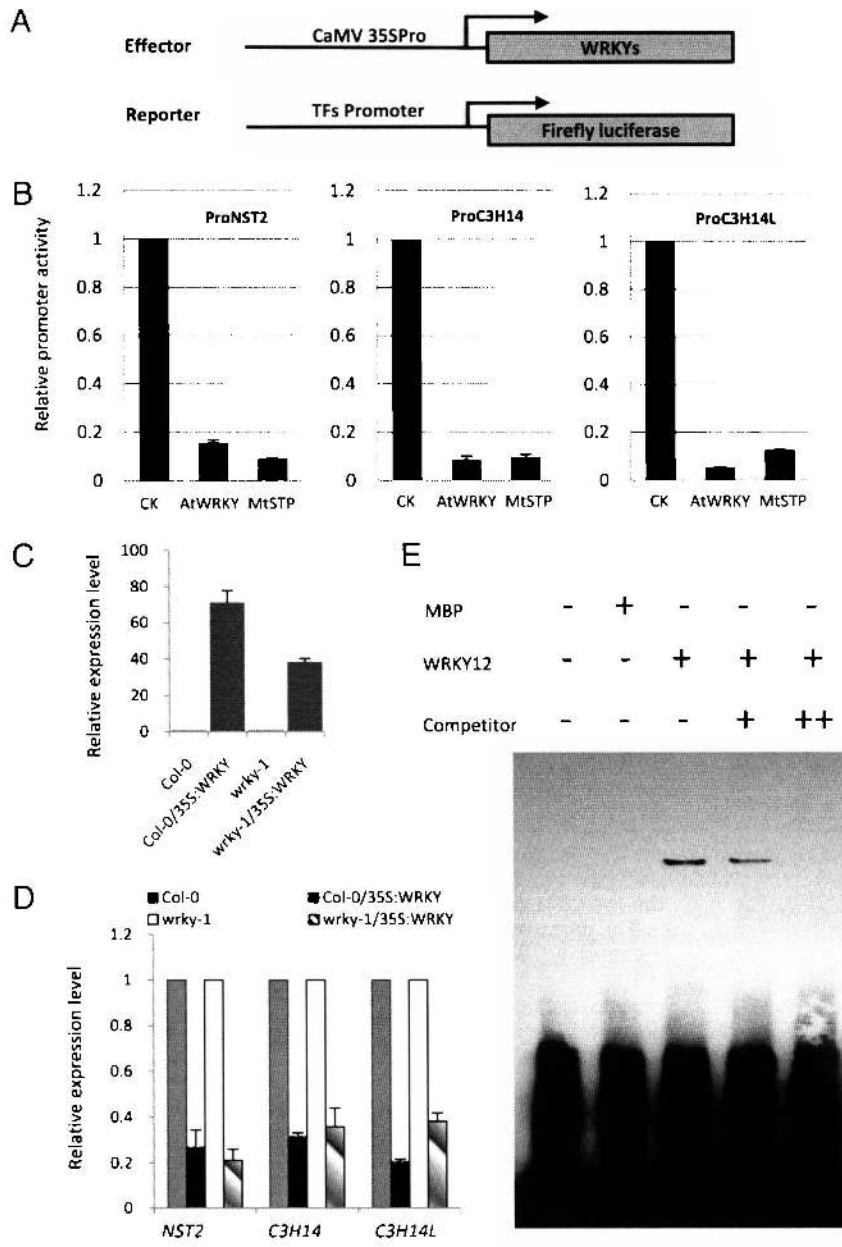


Fig. 4. STP protein represses the expression of downstream transcription factors. (A) Constructs used in transient expression assays. (B) Promoter activity of *NST2*, *C3H14*, and *C3H14L* in *Arabidopsis* leaf protoplasts is repressed by overexpression of *AtWRKY12* or *MtSTP* genes. Error bars represent \pm SD from three independent replicates. (C) Overexpression of *WRKY12* detected by qRT-PCR in WT and *wrky12-1* backgrounds. (D) Repression of *NST2*, *C3H14*, and *C3H14L* transcript levels in *WRKY12* overexpressing lines. Error bars represent SD from three independent replicates. (E) EMSA results showing direct binding of *AtWRKY12* to the *NST2* promoter fragment.

stream master switch of *MYB46* and *MYB83*, rarely causes ectopic secondary wall formation in either cortex or pith cells (5, 9), indicating the existence of a complex transcription regulation network. How and why plants have evolved different mechanisms to control cell wall formation in pith and cortex cells are still open questions.

Many of the *WRKY* genes identified to date are involved in plant defense (27–29). The involvement of *WRKY* genes in lignification so far seems to be limited to potential roles as activators of lignification in response to microbial signals (30). The function of *WRKY* genes as repressors of lignification and other components of the secondary cell wall development program may have evolved to limit wasteful carbon allocation into cells in the stem that are not essential to support the plant against gravity.

Much of the biomass on the Earth's surface is found in plant secondary cell walls. The present observations of large increases in cell wall thickness, stem biomass density, and above-ground biomass resulting from knockout of a single gene suggest a strategy to generate additional cell wall biomass in the stems of dicotyledonous forage and bioenergy crops without otherwise affecting the health and growth habit of the plants. The latter must

still be shown under diverse environmental conditions. It remains to be determined whether similar genetic controls exist in monocotyledonous species.

Materials and Methods

Plant Materials and Growth Conditions. Growth of mutant and WT plants and screening for mutants with altered lignification patterns are described in *SI Materials and Methods*.

Pith Cell Isolation from *M. truncatula* and *Arabidopsis* Plants. To isolate the pith from *M. truncatula*, stems were cut into 2-cm segments, and surrounding fiber and vascular tissues were removed by blade under a stereomicroscope. About 15 main stems from individual plants were used for isolation of pith, which was pooled for lignin analysis, frozen in liquid nitrogen, and stored at -80°C . *Arabidopsis* stems were cut into 0.5-cm segments and fixed immediately on ice in 75% (vol/vol) ethanol and 25% (vol/vol) acetic acid overnight. The fixative was exchanged by 10% (wt/vol) sucrose solution in PBS buffer (137 mM NaCl, 8.01 mM Na_2HPO_4 , 2.68 mM KCl, 1.47 mM KH_2PO_4 , pH 7.3); the mixture was kept at 4°C for 2 h and then exchanged for 15% (wt/vol) sucrose in the same buffer overnight. The segments were longitudinally

sectioned to 60 μm using a Leica CM1850 cryostat and mounted on membrane-coated glass slides (Carl Zeiss MicroImaging). Pith and fiber tissues were then separated using microknives, picked using tweezers together with the membrane, and frozen at -80°C .

Microarray Analysis. This was performed as described in *SI Materials and Methods*.

Immunocytochemistry and Microscopy. Tissue processing and immunolocalization using monoclonal antibodies to recognize various carbohydrate epitopes were carried out as described (21). Monoclonal antibodies were obtained as hybridoma cell culture supernatants from either the Complex Carbohydrate Research Center (JIM and MAC series; available from CarboSource Services; <http://www.carbosource.net>) or PlantProbes (LM series, PAM1; <http://www.plantprobes.net>). The antibodies recognize apparently distinct xylan epitopes as described (21). CBM2a was obtained from Dr. Harry Gilbert (University of Newcastle, Newcastle upon Tyne, United Kingdom), and its immunolabeling required an additional anti-polyhistidine antibody (H-1029; Sigma) step (22). For transmission EM, 80-nm sections were taken and stained with 2% uranyl acetate for 5 min and Reynold's lead citrate (31) for 1 min. Sections were observed under a Zeiss 902A transmission electron microscope operated at 80 kV.

Molecular Cloning of the *MtSTP* Gene. To identify the gene linked to the STP phenotype, candidate genes were chosen based on the extent of down-regulation and stem expression specificity. PCR was performed using the *Tnt1* forward primer 5'-TCCTTGTGGATTGGTAGCCAACCTTGTG-3', the reverse primer 5'-AGTTGGCTACCAATCCAACAAGGA-3', and the gene-specific primers *MtSTP*_F 5'-ATGGATGGAGAAAGAGATGTCC-3' and *MtSTP*_R 5'-TCAAAAAGACGTAAACATTCGTG-3' to detect *Tnt1* insertions.

Real-Time PCR Analysis. This was performed as described in *SI Materials and Methods*.

Protoplast Isolation and trans-Activation Assay. Arabidopsis protoplasts were isolated according to a previously published protocol with minor modifications (32). In brief, leaves from healthy 30-d-old *Arabidopsis* were cut into 0.5- to 1-mm strips with fresh razor blades. The leaf strips were put into a solution of cellulase R10 and macerozyme (Yakult Honsha) and then underwent vacuum infiltration for 5–30 min followed by digestion for 3 h without shaking in the dark. The protoplasts were collected on a 35- to 75- μm nylon mesh and transformed by PEG-mediated transfection. The firefly luciferase construct was modified from a Gateway compatible vector pPGWL7 (33). Promoter activities were represented by Firefly LUC/Renilla LUC activities and normalized to the value obtained from protoplasts transformed with empty vector.

Gene Constructs and Plant Transformation. Complementation of the Arabidopsis *wrky12* mutant was performed as described in *SI Materials and Methods*.

Protein Expression and Electrophoretic Mobility Shift Assays. These were performed as described in *SI Materials and Methods*.

Determination of Lignin Content and Composition. Lignin content of stem material (internodes five to eight) was determined by thioacidolysis, which, together with phloroglucinol and Mäule staining methods, was conducted as described (34).

ACKNOWLEDGMENTS. We thank Drs. Elison Blancaflor and Richard S. Nelson for critical reading of the manuscript and Dr. Yuhong Tang for assistance with microarray analysis. This work was supported by grants from the US Department of Energy (DE-GG02-06ER64303 and DEFS02-06ER64304), the Oklahoma Bioenergy Center (OBC), and the Samuel Roberts Noble Foundation. The BioEnergy Science Center is supported by the Office of Biological and Environmental Research in the Department of Energy Office of Science. Generation of the Complex Carbohydrate Research Center series of monoclonal antibodies used in this research was supported by Grant DBI-0421683 from the National Science Foundation Plant Genome Program, and the *M. truncatula* *Tnt1* mutants, jointly owned by Centre National de la Recherche Scientifique and the Noble Foundation, were created through research funded in part by Grant 703285 from the National Science Foundation.

- Harris D, DeBolt S (2010) Synthesis, regulation and utilization of lignocellulosic biomass. *Plant Biotechnol J* 8:244–262.
- Rubin EM (2008) Genomics of cellulosic biofuels. *Nature* 454:841–845.
- Demura T, Fukuda H (2007) Transcriptional regulation in wood formation. *Trends Plant Sci* 12:64–70.
- Zhong R, Ye ZH (2007) Regulation of cell wall biosynthesis. *Curr Opin Plant Biol* 10:564–572.
- Mitsuda N, et al. (2007) NAC transcription factors, NST1 and NST3, are key regulators of the formation of secondary walls in woody tissues of *Arabidopsis*. *Plant Cell* 19:270–280.
- Mitsuda N, Seki M, Shinozaki K, Ohme-Takagi M (2005) The NAC transcription factors NST1 and NST2 of *Arabidopsis* regulate secondary wall thickenings and are required for anther dehiscence. *Plant Cell* 17:2993–3006.
- Yamaguchi M, Kubo M, Fukuda H, Demura T (2008) Vascular-related NAC-DOMAIN7 is involved in the differentiation of all types of xylem vessels in *Arabidopsis* roots and shoots. *Plant J* 55:652–664.
- Zhao Q, et al. (2010) A NAC transcription factor orchestrates multiple features of cell wall development in *Medicago truncatula*. *Plant J* 63:100–114.
- Zhong R, Demura T, Ye ZH (2006) SND1, a NAC domain transcription factor, is a key regulator of secondary wall synthesis in fibers of *Arabidopsis*. *Plant Cell* 18:3158–3170.
- Steiner-Lange S, et al. (2003) Disruption of *Arabidopsis thaliana* MYB26 results in male sterility due to non-dehiscent anthers. *Plant J* 34:519–528.
- Zhong R, Richardson EA, Ye ZH (2007) The MYB46 transcription factor is a direct target of SND1 and regulates secondary wall biosynthesis in *Arabidopsis*. *Plant Cell* 19:2776–2792.
- Zhong R, Lee C, Zhou J, McCarthy RL, Ye ZH (2008) A battery of transcription factors involved in the regulation of secondary cell wall biosynthesis in *Arabidopsis*. *Plant Cell* 20:2763–2782.
- Zhou J, Lee C, Zhong R, Ye ZH (2009) MYB58 and MYB63 are transcriptional activators of the lignin biosynthetic pathway during secondary cell wall formation in *Arabidopsis*. *Plant Cell* 21:248–266.
- Caño-Delgado AI, Metzclaff K, Bevan MW (2000) The *eli 1* mutation reveals a link between cell expansion and secondary cell wall formation in *Arabidopsis thaliana*. *Development* 127:3395–3405.
- Zhong R, Ripberger A, Ye ZH (2000) Ectopic deposition of lignin in the pith of stems of two *Arabidopsis* mutants. *Plant Physiol* 123:59–70.
- Ellis C, Karafyllidis I, Wasternack C, Turner JG (2002) The *Arabidopsis* mutant *cev1* links cell wall signaling to jasmonate and ethylene responses. *Plant Cell* 14:1557–1566.
- Zhong R, Kays SJ, Schroeder BP, Ye ZH (2002) Mutation of a chitinase-like gene causes ectopic deposition of lignin, aberrant cell shapes, and overproduction of ethylene. *Plant Cell* 14:165–179.
- Tadege M, Ratet P, Mysore KS (2005) Insertional mutagenesis: A Swiss Army knife for functional genomics of *Medicago truncatula*. *Trends Plant Sci* 10:229–235.
- Tadege M, et al. (2008) Large-scale insertional mutagenesis using the *Tnt1* retrotransposon in the model legume *Medicago truncatula*. *Plant J* 54:335–347.
- Lapierre C, Monties B, Rolando C, Chirale DL (1985) Thioacidolysis of lignin: comparison with acidolysis. *J Wood Chem Technol* 5:277–292.
- Pattathil S, et al. (2010) A comprehensive toolkit of plant cell wall glycan-directed monoclonal antibodies. *Plant Physiol* 153:514–525.
- Blake AW, et al. (2006) Understanding the biological rationale for the diversity of cellulose-directed carbohydrate-binding modules in prokaryotic enzymes. *J Biol Chem* 281:29321–29329.
- Benedito VA, et al. (2008) A gene expression atlas of the model legume *Medicago truncatula*. *Plant J* 55:504–513.
- Alonso JM, et al. (2003) Genome-wide insertional mutagenesis of *Arabidopsis thaliana*. *Science* 301:653–657.
- Ko JH, Kim WC, Han KH (2009) Ectopic expression of MYB46 identifies transcriptional regulatory genes involved in secondary wall biosynthesis in *Arabidopsis*. *Plant J* 60:649–665.
- McCarthy RL, Zhong R, Ye ZH (2009) MYB83 is a direct target of SND1 and acts redundantly with MYB46 in the regulation of secondary cell wall biosynthesis in *Arabidopsis*. *Plant Cell Physiol* 50:1950–1964.
- Eulgem T (2006) Dissecting the WRKY web of plant defense regulators. *PLoS Pathog* 2:e126.
- Eulgem T, Somssich IE (2007) Networks of WRKY transcription factors in defense signaling. *Curr Opin Plant Biol* 10:366–371.
- Zheng Z, Mosher SL, Fan B, Klessig DF, Chen Z (2007) Functional analysis of *Arabidopsis* WRKY25 transcription factor in plant defense against *Pseudomonas syringae*. *BMC Plant Biol* 7:2–15.
- Naoumkina MA, He X, Dixon RA (2008) Elicitor-induced transcription factors for metabolic reprogramming of secondary metabolism in *Medicago truncatula*. *BMC Plant Biol* 8:132–146.
- Reynolds ES (1963) The use of lead citrate at high pH as an electron-opaque stain in electron microscopy. *J Cell Biol* 17:208–212.
- Asai T, et al. (2002) MAP kinase signalling cascade in *Arabidopsis* innate immunity. *Nature* 415:977–983.
- Karimi M, Inzé D, Depicker A (2002) GATEWAY vectors for Agrobacterium-mediated plant transformation. *Trends Plant Sci* 7:193–195.
- Guo D, Chen F, Inoue K, Blount JW, Dixon RA (2001) Downregulation of caffeoyl 3-O-methyltransferase and caffeoyl CoA 3-O-methyltransferase in transgenic alfalfa, impacts on lignin structure and implications for the biosynthesis of G and S lignin. *Plant Cell* 13:73–88.